symmetry

MDPI

*Article*

# Wave Propagation in Shear Beams Comprising Finite Periodic Lumped Masses and Resting on Elastic Foundation

**Aydin Ozmutlu**

Department of Civil Engineering, Corlu Engineering Faculty, Tekirdag Namik Kemal University, Tekirdag 59860, Turkey; aozmutlu@nku.edu.tr

**Abstract:** In this study, the dispersion of an infinite shear beam with a lumped mass connected at periodic distances and resting on an elastic foundation was examined. The effect of periodicity in the finite region of the lumped masses on wave propagation was investigated through a one-dimensional model. The dispersion relationship for Bragg scattering, which consists of one-dimensional periodic lumped masses, was derived using the transfer matrix method. Subsequently, to evaluate the effect of parameters such as the magnitude of the lumped mass and foundation stiffness on the dynamic response of the shear beam, several simulations were performed. The band frequency characteristics of the shear beam are demonstrated with respect to the variations in stiffness and mass. Using the wave-based approach, the effect of periodic masses on wave propagation in a finite region of an infinite beam was revealed. Periodic masses have been shown to have a positive effect on the displacement amplitude; in other words, a lumped mass barrier is effective in providing wave attenuation.

**Keywords:** wave dispersion; periodic structure; lumped mass; band gap; wave barrier; elastic foundation



**Citation:** Ozmutlu, A. Wave Propagation in Shear Beams Comprising Finite Periodic Lumped Masses and Resting on Elastic Foundation. *Symmetry* **2023**, *15*, 17. https://doi.org/10.3390/sym15010017

Academic Editor: Dumitru Baleanu

Received: 4 November 2022
Revised: 9 December 2022
Accepted: 14 December 2022
Published: 21 December 2022



## 1. Introduction

Recently, the mechanical behavior of periodic structures has attracted increasing attention from researchers. When the frequency spectrum of these structures is examined, a banded formation is observed [1]. Both the material and the structure periodicity lead to wave dispersion in such systems, where wave propagation does not occur at a certain frequency range. This pattern of behavior, unique to periodicity, is beneficial for eliminating the source of vibrations caused by dynamic effects in structures or reducing the effects of vibrations.

Periodic structures can be defined as systems consisting of more than one identical component [2]. Beams composed of identical structural members connected in the form of beam segment-lumped mass introduce features of a periodic structure. When studies in the literature are reviewed, it is observed that mathematical techniques for the solution of periodic structure problems (crystal lattice structures, periodic electrical circuits, continuous transmission lines) have been developed since the beginning of the 20th century. Brillouin investigated and analyzed the crystal lattice structure and periodic electrical circuit problems and also explained the historical background of the subject in detail [3].

Examining simple models while explaining a physical problem is a commonly preferred method. In this study, the propagation of elastic waves along a beam with periodic masses is investigated through a simple beam model that explained only the shear deformation of the structure as a whole and the scattering of waves from lumped masses. This established model aims to provide an insight into how periodic mass distribution affects wave propagation. This model corresponds to a periodic structure that can be considered a (1D) phononic crystal (PC) [1,2,4–6]. The formation mechanism of the band gap, which results from structural periodicity (discontinuities) in the model, is based on wave interference and Bragg scattering [7,8]. Therefore, the interference of incident waves and the waves

scattered from masses can be analyzed within the framework of Bragg scattering [9]. The interaction between the incident and reflected waves produces constructive/destructive interference [7,9,10]. Goto et al. [11] numerically investigated the forced vibrations and Bragg scattering of a PC rod within the framework of higher-order rod theories and verified them with experimental results. Santos et al. [12] focused on the transmission of bending vibrations between a finite number of periodic cells and an infinite periodic beam.

Periodic beams have been the subject of various studies; however, studies on periodic beams resting on an elastic foundation are limited in the literature [13]. In preliminary work on this subject [14], bending wave propagation in an infinitely periodic Euler–Bernoulli beam resting on an elastic foundation was investigated using the Floquet theory. Yu et al. [15] investigated the dispersion properties of the bending wave in infinitely long beams with different periodic states and examined the effects of the elastic foundation on the band gap. Han et al. [16] analyzed the frequency distribution relationship and frequency response of beam foundation systems with hinged-joint periodicity and showed that the presence of hinges greatly helps to achieve both lower and wider bandwidths with stronger attenuation. Xiang and Shi [17] investigated the bending vibrations of binary periodic beams on a Pasternak foundation and proposed a structural design to attenuate the vibrations. Liu and Shi [18] examined wave propagation in periodic beams resting on a nonlinear elastic foundation with a new perturbation approach and showed that it can be used in the analysis of nonlinear periodic structures (such as buried pipelines and strip foundations). In another study, dynamic problems of periodic Timoshenko beams resting on a two-parameter elastic foundation were investigated with the same method [19]. Ding et al. [20] investigated the effect of foundation parameters on the dispersion behavior of an infinite biperiodic rods resting on a viscoelastic foundation.

Researchers have developed a variety of methods to reveal the band gap characteristics in periodic structures and to ascertain the dispersion relationship. The transfer matrix method (TMM) method is one of the most commonly used methods to reveal the dynamic behavior of periodic structures and PCs [21–23]. The TMM was used to obtain the dispersion relationship observed in the wave propagation problems of both periodic rods and beams [6,11,24–27]. In the TMM, which is used to model the periodic unit cell, the model is reduced to an eigenvalue problem, and it is thus possible to obtain wave numbers and dispersion curves. However, the TMM alone is not sufficient for the analysis of wave propagation problems. Reflected and transmitted waves at structural discontinuities such as hinges, resonators, and boundaries along structural members can be analyzed with the wave-based (WB) approach. Various discontinuity situations [28,29] and elastic foundation effects [30] for different beam theories were investigated with this method. In periodic structures (especially in complex lattice structures), wave propagation properties were investigated by using the TMM and WB approach together [31]. In addition, this approach has been used to investigate wave propagation in 1D and two-dimensional (2D) periodic structures to find natural frequencies and mode shapes [32,33]. The wave-based transfer matrix method has also shown wide applicability in other studies to analyze the dynamic response of large mesh structures [34] to solve the nonlinear vibration problem [35] and to provide necessary vibration controls in the design and analysis of light beams [36–38].

In this study, the effect of wave propagation and finite periodicity on dispersion was investigated in an infinitely long shear beam (SB) with lumped mass connected at periodic distances in a finite region. The vibrations of a structure due to seismic effects from the ground can be reduced by artificially placing lumped masses in a periodic way. Thus, the main purpose of this research is to look into the effects of periodicity in the finite region of an infinite beam resting on an elastic foundation. The transfer matrix (TM) for the beam segment is derived from the solution of the governing equation, and the TM for the lumped mass is obtained using the dynamic equilibrium and displacement conditions. Using the derived TMs, the generalized transfer matrix (GTM) for the periodic unit cell was obtained by a matrix multiplication operation. In the infinite beam, the transmission function (barrier effect of periodic masses) and mode shapes in the finite region are determined by a wave-

based approach. With the wave-based approach, the relationships between two uniform beam sections and unknown wave coefficients are obtained by analyzing the reflection and transmission of waves at discontinuities. Finally, the effect of periodic masses on the wave propagation in a shear beam in a finite region, in other words, the barrier effect, is presented.

## 2. Model and Solution Method

In this section, the dynamic stiffness matrix (DSM), responding to the structure in the frequency domain, was obtained through the solution of the wave equation to determine the dynamic behavior in the model discussed. Unlike the stiffness matrix (SM) used in the conventional finite element method (FEM), it was obtained analytically by deriving it from the solution of the governing equation of an element. The pioneering studies on the application of the DSM to wave propagation problems were conducted by Doyle [39].

The TM obtained using the DSM for a shear beam with a periodic lumped mass provides the exact solution of the dispersion relationship. To this end, the field transfer matrix (FTM) was first derived for the shear beam, and then the GTM was obtained using the PTF written for lumped masses.

Let us discuss the harmonic wave motion in an infinite shear beam with periodic lumped masses presented in Figure 1. This beam is periodic in terms of material, geometry, boundary condition, and spatial variation of the lumped mass along its axis. It was assumed that there was a perfect adhesion between the lumped masses and the beam parts that constituted this system. This beam, in which deformations depend only on shear force $V(x,t)$, has $\rho$ material density and $G$ shear modulus, and $m$ lumped masses are periodically repeated at $\ell$ intervals.

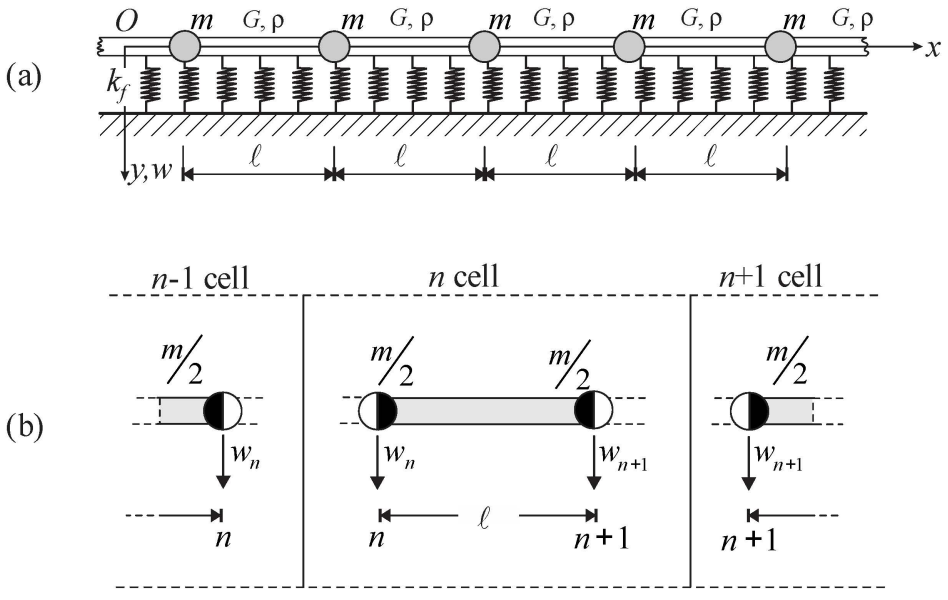


**Figure 1.** Analytical Model: (**a**) Shear beam with periodic lumped masses on the elastic foundation; (**b**) unit periodic cell.

The free-body diagram of a differential element taken in the beam part during the deformation under the effect of shear force is shown in Figure 2a.

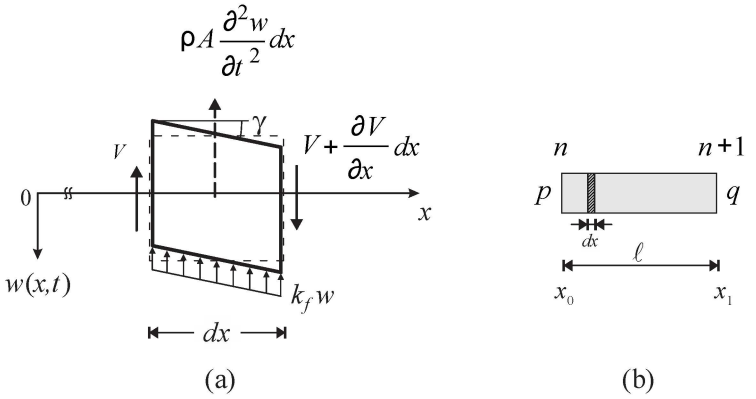


**Figure 2.** (**a**) Free-body diagram of the deformed element; (**b**) Nodal points for the $n$th beam part.

The equation of motion for the shear beam on the elastic foundation is as follows [40]:

$$\frac{\partial V}{\partial x} - k_f w = \rho A \frac{\partial^2 w}{\partial t^2} \tag{1}$$

where $w(x,t)$ is the vertical displacement, and $A$ is the cross-sectional area of the beam. In the study, one parameter foundation model is used and $k_f$ is the foundation parameter. The constitutive equation is written as shown below:

$$V = \kappa G A \frac{\partial w}{\partial x} \tag{2}$$

where $\kappa$ is a quantity depending on the cross-sectional shape and is called the shear correction factor, and $G$ is the shear modulus. If Equation (2) is written in its place in Equation (1), the wave equation of the shear beam is obtained as follows:

$$\frac{\partial^2 w}{\partial x^2} = \bar{k}_f w + \frac{1}{\beta^2}\frac{\partial^2 w}{\partial t^2} \tag{3}$$

where $\bar{k}_f = k_f/\kappa GA$, $\beta = c_S\sqrt{\kappa}$ and $c_S = \sqrt{G/\rho}$ is the shear wave velocity in the medium. By assuming that the time dependence of the behavior of the medium is harmonic in the form of $e^{-i\omega t}$, where $\omega$ = circular frequency, then the time dependence of force and displacement can be taken as $V(x,t) = \overline{V}(x)e^{-i\omega t}$ and $w(x,t) = W(x)e^{-i\omega t}$, respectively. In this case, the solution of the wave equation is obtained as follows:

$$W(x) = C_1 e^{ir_1 x} + C_2 e^{ir_2 x} \tag{4}$$

where $i$ is the imaginary unit and the characteristic roots are $r_{1,2} = \pm\sqrt{(\omega/\beta)^2 - \bar{k}_f}$. For wave propagation to occur, the square root expression must be positive. In this case, it should be $\omega > \omega_{cr} = \sqrt{k_f/\rho A}$. Where $\omega_{cr}$ is the cut-off frequency and below this value, the waves cannot propagate in an undamped system.

According to the situation in Figure 2b, the end displacements and forces can be written as follows. Here, in the beam part, the end $n$ is specified as node $p$, and the end $n+1$ is specified as node $q$.

$$x = x_0: \qquad w(x_0) = W_p \text{ and } \overline{V}_p = \overline{V}(x_0) = -\kappa GA \left.\frac{dW}{dx}\right|_{x=x_0} \tag{5}$$

$$x = x_0 + \ell = x_1: \qquad w(x_1) = W_q \text{ and } \overline{V}_q = \overline{V}(x_1) = \kappa GA \left.\frac{dW}{dx}\right|_{x=x_1} \tag{6}$$

If the wave solution is substituted in Equations (5) and (6) and arranged in the matrix form, the following relations are obtained:

$$\begin{Bmatrix} W_p \\ W_q \end{Bmatrix} = \begin{bmatrix} e^{ir_1x_0} & e^{ir_2x_0} \\ e^{ir_1x_1} & e^{ir_2x_1} \end{bmatrix} \begin{Bmatrix} C_1 \\ C_2 \end{Bmatrix} \tag{7}$$

$$\begin{Bmatrix} \overline{V}_p \\ \overline{V}_q \end{Bmatrix} = i\kappa GA \begin{bmatrix} -r_1e^{ir_1x_0} & -r_2e^{ir_2x_0} \\ r_1e^{ir_1x_1} & r_2e^{ir_2x_1} \end{bmatrix} \begin{Bmatrix} C_1 \\ C_2 \end{Bmatrix} \tag{8}$$

The DSM $\mathbf{S}_t$, which gives the relationship between shear forces and displacements, is obtained by eliminating the coefficients $C_1$ and $C_2$ from Equations (7) and (8) [41,42]. In this case, the force-displacement vector relationship is as follows:

$$\begin{Bmatrix} \overline{V}_p \\ \overline{V}_q \end{Bmatrix} = \mathbf{S}_2\mathbf{S}_1^{-1} \begin{Bmatrix} W_p \\ W_q \end{Bmatrix} \tag{9}$$

where $\mathbf{S}_t = \mathbf{S}_2\mathbf{S}_1^{-1}$ is the DSM, $\mathbf{S}_1$ and $\mathbf{S}_2$ are spectral matrices obtained from geometric and dynamic boundary conditions [39].

### *2.1. Field Transfer Matrix for the Beam Segment*

The transition from the DSM to the FTM is possible because DSM is related to FTM. Once the stiffness matrix of the beam segment is obtained, the corresponding transfer matrix can be computed. Due to the dynamic FTM, if the section forces and displacements (input end) of a beam at one end are known, the section forces and displacements (output end) at the other end can be found.

The FTM establishes the following relationship between the state vectors at ends $p$ and $q$ of any beam part [43]:

$$\mathbf{f}(x_1) = \mathbf{T}_b(x_1, x_0)\, \mathbf{f}(x_0) \tag{10}$$

where $\mathbf{f}(x_0)$ is the initial state vector and defines the input end $\left\{W_0, \overline{V}_0\right\}^T$, and $\mathbf{f}(x_1)$ is the final state vector and defines the output end $\left\{W_1, \overline{V}_1\right\}^T$. $\mathbf{T}_b(x_1, x_0)$ is the FTM and a matrix operator that performs the linear transformation between the domain and the target space. The following relationships exist between the elements of this matrix and the elements of the DSM:

$$\begin{aligned} \mathbf{T}_{b11} &= -\mathbf{S}_{t11}\mathbf{S}_{t12}^{-1} \\ \mathbf{T}_{b12} &= -\mathbf{S}_{t12}^{-1} \\ \mathbf{T}_{b21} &= \mathbf{S}_{t21} - \mathbf{S}_{t22}\mathbf{S}_{t11}\mathbf{S}_{t12}^{-1} \\ \mathbf{T}_{b22} &= -\mathbf{S}_{t22}\mathbf{S}_{t12}^{-1} \end{aligned} \tag{11}$$

The explicit expression of the dynamic FTM is shown below:

$$\mathbf{T}_b = \begin{bmatrix} \cos[r_1(x_1 - x_0)] & \frac{1}{\kappa GAr_1}\sin[r_1(x_1 - x_0)] \\ -\kappa GAr_1 \sin[r_1(x_1 - x_0)] & \cos[r_1(x_1 - x_0)] \end{bmatrix} \tag{12}$$

### *2.2. Point Transfer Matrix for the Lumped Mass*

The PTM for the lumped mass will be written over the dynamic equilibrium equation and continuity conditions. The free-body diagram of the lumped mass at the boundary between any cell $n$ and $n + 1$, namely, at the point $x = x_n$, and the section forces acting on it and the inertia force is presented in Figure 3.

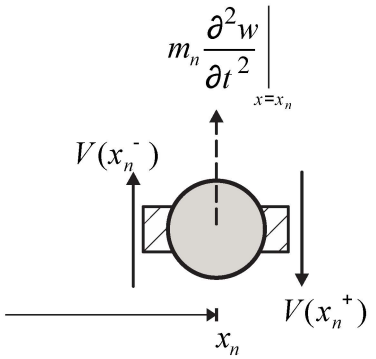


**Figure 3.** Free-body diagram for the lumped mass at the point $x = x_n$.

At this stage, it has been assumed that there is perfect bonding between the adjacent SB segments and the lumped mass. First, if the dynamic equilibrium condition is written to obtain the PTM, the following relation is obtained:

$$V(x_n{}^+) = V(x_n{}^-) + m_n \ddot{w}(x_n{}^-) \tag{13}$$

where $m_n$ is the lumped mass at point $n$. Second, the displacement condition is as follows:

$$w(x_n{}^+) = w(x_n{}^-) = w(x_n) \tag{14}$$

If the time-harmonic dependency $e^{-i\omega t}$ is omitted and rearranged in Equations (13) and (14) above, the following relationship is written between the state vectors and the PTM:

$$\mathbf{f}(x_n{}^+) = \mathbf{T}_p(x_n)\mathbf{f}(x_n{}^-) \tag{15}$$

where $\mathbf{T}_p(x_n)$ is the PTM at the $x = x_n$ boundary, and its explicit expression is presented below:

$$\mathbf{T}_p(x_n) = \begin{bmatrix} 1 & 0 \\ -\omega^2 m_n & 1 \end{bmatrix} \tag{16}$$

*2.3. Generalized Transfer Matrix and Dispersion Equation for the Periodic Cell*

The FTM in the beam segment and the PTM for the lumped mass at the boundary were obtained. If these matrices are written from the start point to the end point for a finite beam, the generalized transfer matrix for the unit cell is obtained.

$$\mathbf{f}(x_0 + \ell) = \mathbf{T}_c(\ell)\mathbf{f}(x_0) \tag{17}$$

In general, a periodic cell (lumped masses and beam part) consists of two-point propagation matrices and one field propagation matrix.

$$\mathbf{T}_c(\ell) = \mathbf{T}_p(m/2)\mathbf{T}_b(\ell)\mathbf{T}_p(m/2) \tag{18}$$

The unit cell forms a periodic structure that repeats itself at $\ell$ distance. The state vector along this $n$ cell periodic structure is written as follows:

$$\mathbf{f}(x_0 + n\ell) = \mathbf{T}_c^n(\ell)\mathbf{f}(x_0), \quad n = \pm 1, \pm 2, \ldots \tag{19}$$

The periodic boundary conditions for the steady-state solution of the discussed infinitely long shear beam are written in the following way:

$$\mathbf{f}(x_0 + n\ell) = \mathbf{f}(x_0), \quad n = \pm 1, \pm 2, \ldots \tag{20}$$

If the behavior concerning time is harmonic due to periodicity, it can be written using the Floquet–Bloch theorem [3].

$$\mathbf{f}(x_0 + n\ell) = e^{ik_c n\ell}\mathbf{f}(x_0) \tag{21}$$

where $k_c$ is the wave number for the beam segment and the entire periodic structure it forms. The $\mathbf{T}_c^n(\ell)$ matrix is the same in every cell of structures that are entirely periodic. Therefore, $n = 1$ is taken, and the eigenvalue problem of the transfer matrix is obtained using Equations (19) and (21).

$$\det\Big(\mathbf{T}_c(\ell) - e^{ik_c\ell}\mathbf{I}\Big) = 0 \tag{22}$$

The eigenvalues and eigenvectors for the periodic cell can be calculated from Equation (22), where $\Lambda_{c,12} = e^{\pm ik_c\ell}$ are the eigenvalues for the periodic cell. This equation gives the dispersion relation, which shows that the wave propagates differently at each frequency. When the eigenvalues of the transfer matrix are computed, the wave numbers required to find the wave phase velocities are obtained. The wave number for the periodic beam segment is found using Equation (23):

$$k_c = \frac{1}{\ell}\arg(\Lambda_{c,12}) \tag{23}$$

When the $k_c$ values found are examined, it is observed that they do not take continuous values. Certain frequency values which $k_c$ takes continuous values are called the allowed wave number values. The bands in the wave number spectrum are the result of the interference of the waves scattered from different masses.

The allowed $k_c$ values are found by applying the periodic boundary conditions (BC's) (20). The periodic BC's lead to the following equation, which may be derived from Equation (21) by applying the Floquet–Bloch theorem:

$$k_c = j2\pi/\ell, \quad j = \pm 1, 2, \ldots \tag{24}$$

Accordingly, the allowed $k_c$ values given by Equation (24) repeat themselves with period $2\pi/\ell$ and form a lattice in the wave number space. Furthermore, if $k_c$ is the allowed wave number, $k_c \pm j2\pi/\ell, \quad j = 1, 2, \ldots$ is also an allowed wave number. If we define the prime value $k_c$ in the $\left(-\frac{\pi}{\ell}, \frac{\pi}{\ell}\right)$ interval to be symmetrical for $k_c = 0$, this definition interval is called the 1st Brillouin zone. Thus, the wave propagation of an infinitely long periodic beam can be examined. Furthermore, dispersion curves can be obtained by changing the number of waves in the 1st Brillouin zone.

## 3. Wave Motion in the Finite Periodic Region

A formulation of the presence of periodic lumped masses in a 1D finite region, the investigation of their barrier effect, the achievement of the transmission function (TF), and the computation of displacement amplitudes associated with the wave motion are presented in this section. To this end, the expressions required to describe the wave motion in such a medium were first obtained.

### *3.1. Relationship between the State Vector and the Wave Coefficients*

In a homogeneous shear beam on the linear elastic foundation, the relationship between the state vector $\mathbf{f}(x)$ and the wave coefficients $\boldsymbol{a}$ is desired to be established (Figure 4). In this case, the displacement and shear force can be written in the following way:

$$w(x,t) = \Big(A_+ e^{ik_s x} + A_- e^{-ik_s x}\Big)e^{-i\omega t} \tag{25}$$

$$V(x,t) = ik_s(\kappa GA)\Big(A_+ e^{ik_s x} - A_- e^{-ik_s x}\Big)e^{-i\omega t} \tag{26}$$

where $A_+$ and $A_-$ are complex wave coefficients, $A_+e^{ik_sx-i\omega t}$ and $A_-e^{-ik_sx-i\omega t}$ are harmonic waves propagating in the positive and negative $x$-directions, respectively. When the solution of the wave equation is obtained, it is seen that the characteristic roots of $r_{1,2} = \pm ik_s$ correspond to the wave number, $k_s$.

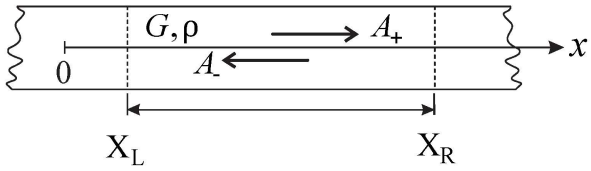


**Figure 4.** Wave propagation between the defined boundaries.

Generally, the state vector is written for the steady-state solutions as follows:

$$\mathbf{f}(x) = \mathbf{X}\mathbf{\Lambda}(x)\boldsymbol{a} \tag{27}$$

The expressions used in Equation (27) here,

$$\begin{aligned} \mathbf{X} &= \begin{bmatrix} 1 & 1 \\ ik_s(\kappa GA) & -ik_s(\kappa GA) \end{bmatrix} \\ \mathbf{\Lambda}(x) &= \begin{bmatrix} e^{ik_sx} & 0 \\ 0 & e^{-ik_sx} \end{bmatrix} \\ \boldsymbol{a} &= \{A_+, A_-\}^T \end{aligned} \tag{28}$$

Now, let us establish the relationship between the state vectors and wave coefficients defined at two points, such as $x = \mathrm{X_L}$ and $x = \mathrm{X_R}$, defined in the same medium (Figure 4).

The wave coefficients can be uniquely determined from the two given boundary conditions. Let us assume that the state vector at point $x = \mathrm{X_L}$ is $\mathbf{f}(\mathrm{X_L})$ and that it is known. Then, it can be written in the following way:

$$\mathbf{f}(\mathrm{X_L}) = \mathbf{X}\mathbf{\Lambda}(\mathrm{X_L})\boldsymbol{a} \tag{29}$$

If the state vector $\mathbf{f}(\mathrm{X_R})$ at point $x = \mathrm{X_R}$ is calculated, the following expression is obtained:

$$\begin{aligned} \mathbf{f}(\mathrm{X_R}) &= \mathbf{X}\mathbf{\Lambda}(\mathrm{X_R})\boldsymbol{a} \\ &= \mathbf{X}\mathbf{\Lambda}(\mathrm{X_R} - \mathrm{X_L})\mathbf{X}^{-1}\mathbf{f}(\mathrm{X_L}) \end{aligned} \tag{30}$$

where $\mathbf{\Lambda}(\mathrm{X_R} - \mathrm{X_L}) = diag\left\{e^{ik_s(\mathrm{X_R}-\mathrm{X_L})}, e^{-ik_s(\mathrm{X_R}-\mathrm{X_L})}\right\}$, or it can also be written as follows:

$$\mathbf{f}(\mathrm{X_R}) = \mathbf{T}_b(\mathrm{X_R} - \mathrm{X_L})\ \mathbf{f}(\mathrm{X_L}) \tag{31}$$

where $\mathbf{T}_b(\mathrm{X_R} - \mathrm{X_L})$ is the matrix that moves the state vector at point $x = \mathrm{X_L}$ from left to right in the same medium.

### *3.2. Reflection and Transmission at the Boundary*

Now, let us examine the situation where the properties of the medium to the right and left of a point like $x = \mathrm{X_B}$ are the same, and there is a lumped mass $m$ at the boundary (Figure 5). At this point, let us assume that the wave coming from the left medium and crossing the boundary is not reflected from the right medium (the absorbing boundary condition). By Sommerfeld's radiation condition, if no other obstacles are present, the waves continue to propagate (outgoing waves) to infinity but do not return from infinity.

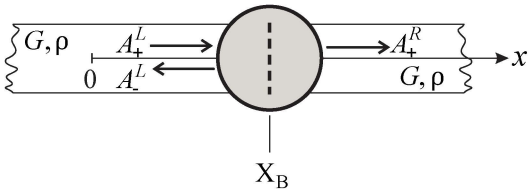


**Figure 5.** Waves passing through the boundary and reflected at point $x = X_B$.

Let us define the displacement vectors in the left and right media, respectively.

$$x < X_B{}^- : \qquad W(x) = A_+^L e^{ik_s x} + A_-^L e^{-ik_s x} \tag{32}$$

$$x > X_B{}^+ : \qquad W(x) = A_+^R e^{ik_s x} \tag{33}$$

The dynamic and geometric boundary conditions will be written to find the transmission and reflection coefficients. The state vector for $x = X_B{}^-$ to the infinitesimal left of the boundary is written as follows:

$$\mathbf{f}(X_B{}^-) = \mathbf{X}\mathbf{\Lambda}(X_B{}^-)\boldsymbol{a}^L \tag{34}$$

and the state vector for $x = X_B{}^+$ to the infinitesimal right is written in the following way:

$$\mathbf{f}(X_B{}^+) = \mathbf{X}\mathbf{\Lambda}(X_B{}^+)\boldsymbol{a}^R \tag{35}$$

where $\boldsymbol{a}^L = \left\{A_+^L, A_-^L\right\}^T$ and $\boldsymbol{a}^R = \left\{A_+^L, 0\right\}^T$ are the wave coefficients vectors of the medium to the left and right of the boundary, respectively. The lumped mass is taken into account while writing the continuity conditions at the boundary.

If the continuity condition relations are given by Equations (13) and (14) are used, a relation between the wave coefficient vectors is obtained as follows:

$$\boldsymbol{a}^R = \left[\mathbf{\Lambda}(X_B{}^+)\right]^{-1}[\mathbf{X}]^{-1}\mathbf{T}_p(X_B)[\mathbf{X}]\left[\mathbf{\Lambda}(X_B{}^-)\right]\boldsymbol{a}^L \tag{36}$$

This relation can also be written in the following way:

$$\boldsymbol{a}^L = \overline{\mathbf{T}}(X_B)\boldsymbol{a}^R \tag{37}$$

where,

$$\overline{\mathbf{T}}(X_B) = \left\{\left[\mathbf{\Lambda}(X_B{}^+)\right]^{-1}[\mathbf{X}]^{-1}\mathbf{T}_p(X_B)[\mathbf{X}]\left[\mathbf{\Lambda}(X_B{}^-)\right]\right\}^{-1} \tag{38}$$

is the transmission matrix of wave coefficient vectors from right to left. Equation (37) is valid at any boundary, regardless of the absorbing boundary conditions. Now, let us find the reflection and transmission coefficients using Equation (37) at a lumped mass boundary (for the absorbing boundary assumption).

$$\alpha^{tran} = \frac{A_+^R}{A_+^L} = \frac{1}{\overline{\mathrm{T}}_{11}} \tag{39}$$

$$\alpha^{ref} = \frac{A_-^L}{A_+^L} = \frac{\overline{\mathrm{T}}_{21}}{\overline{\mathrm{T}}_{11}} \tag{40}$$

where $\alpha^{tran}$ is the transmission coefficient, $\alpha^{ref}$ is the reflection coefficient.

### *3.3. Barrier Effect of Periodic Lumped Masses*

At this stage, let us assume that $\eta_{mass}$ finite number of lumped masses are periodically connected on a beam with unchanged material properties at $\ell$ (the distance between the centers of mass) intervals (Figure 6).

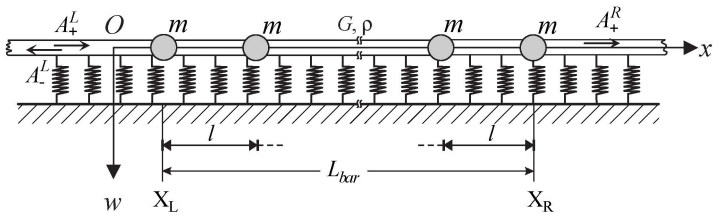


**Figure 6.** Lumped mass barrier.

Let us find the transmission function $H_{bar}(\omega)$ along the barrier. The length of the barrier $L_{bar}$ can be calculated as follows depending on the mass number:

$$L_{bar} = {X_R}^+ - {X_L}^- = (\eta_{mass} - 1)\ell \tag{41}$$

where ${X_L}^-$ is the $x$-coordinate of the point to the infinitesimal left of the first mass, and ${X_R}^+$ is the $x$-coordinate of the point to the infinitesimal right of the last mass. Let the wave coefficient vector be $\boldsymbol{a}^L = \left\{A_+^L, A_-^L\right\}^T$ in the beam to the left of the 1st mass in the barrier, and let the wave coefficient vector be $\boldsymbol{a}^R = \left\{A_+^R, 0\right\}^T$ in the beam to the right of the last mass. The state vector at point $x = {X_L}^-$ is as follows:

$$\mathbf{f}({X_L}^-) = \mathbf{X}\boldsymbol{\Lambda}({X_L}^-)\boldsymbol{a}^L \tag{42}$$

and the state vector at point $x = {X_R}^+$ is written in the following way:

$$\mathbf{f}({X_R}^+) = \mathbf{X}\boldsymbol{\Lambda}({X_R}^+)\boldsymbol{a}^R \tag{43}$$

If the relation between the state vectors $\mathbf{f}({X_L}^-)$ and $\mathbf{f}({X_R}^+)$ is established by the transfer matrix, the following Equation (44)

$$\begin{aligned} \mathbf{f}({X_R}^+) &= \mathbf{f}({X_L}^- + (\eta_{mass} - 1)\ell) \\ &= \mathbf{T}_p(m/2)[\mathbf{T}_c(\ell)]^{(\eta_{mass}-1)}\mathbf{T}_p(m/2)\mathbf{f}({X_L}^-) \end{aligned} \tag{44}$$

can be written more simply as follows:

$$\mathbf{f}\left({X_R}^+\right) = \mathbf{T}_{bar}\mathbf{f}\left({X_L}^-\right) \tag{45}$$

where $\mathbf{T}_{bar} = \mathbf{T}_p(m/2)[\mathbf{T}_c(\ell)]^{(\eta_{mass}-1)}\mathbf{T}_p(m/2)$ is the barrier transfer matrix and contains the information carried by the state vector along the barrier. The relationship between the wave vectors before and after the barrier can be obtained in the following way:

$$\begin{aligned} \boldsymbol{a}^R &= [\boldsymbol{\Lambda}({X_R}^+)]^{-1}[\mathbf{X}]^{-1}\mathbf{f}({X_R}^+) \\ &= [\boldsymbol{\Lambda}({X_R}^+)]^{-1}[\mathbf{X}]^{-1}\mathbf{T}_{bar}\mathbf{X}\boldsymbol{\Lambda}({X_L}^-)\ \boldsymbol{a}^L \end{aligned} \tag{46}$$

This expression can be written as follows:

$$\boldsymbol{a}^R = \mathbf{I}_{bar}\boldsymbol{a}^L \tag{47}$$

where $\mathbf{I}_{bar} = [\boldsymbol{\Lambda}({X_R}^+)]^{-1}[\mathbf{X}]^{-1}\mathbf{T}_{bar}\mathbf{X}\boldsymbol{\Lambda}({X_L}^-)$ is the transmission matrix of the wave coefficient vectors from left to right. Now let us find the wave coefficients for the waves passing through the barrier and reflected.

$$A_-^L = -\frac{I_{bar}(2,1)}{I_{bar}(2,2)}A_+^L \tag{48}$$

$$A_+^R = I_{bar}(1,1) - \frac{I_{bar}(1,2)\cdot\ I_{bar}(2,1)}{I_{bar}(2,2)}A_+^L \tag{49}$$

The transmission function, which gives the amplitude and phase relationship between the wave coming to the barrier and passing through it, can be calculated using these coefficients.

$$H_{bar}(\omega) = \frac{w^{out}}{w^{in}} = \frac{A_+^R}{A_+^L} e^{ik(X_R - X_L)} \tag{50}$$

where $w^{in}$ and $w^{out}$ are the input and output displacements in the beam before and after the barrier, respectively. The frequency band of a periodic structure and a finite periodic structure can be compared using Equation (50).

Now, let us obtain the displacement amplitudes along the barrier. The coefficient functions of structures within the barrier can be calculated recursively based on the relationship between the coefficients to the left and right of a boundary point, such as $x = \mathrm{X_L}$. The coefficient function and displacement in the first unit cell inside the barrier are obtained in the following way:

$$\boldsymbol{a}^{(1)} = \left[\boldsymbol{\Lambda}(\mathrm{X_L}^+)\right]^{-1} [\mathbf{X}]^{-1} \mathbf{T}_p(\mathrm{X_L}) [\mathbf{X}] \left[\boldsymbol{\Lambda}(\mathrm{X_L}^-)\right] \boldsymbol{a}^L \tag{51}$$

$$X_L{}^+ < x < X_L{}^- + d: \qquad W(x) = \boldsymbol{a}^{(1)}(1,1) e^{ik_s x} + \boldsymbol{a}^{(1)}(2,1) e^{-ik_s x} \tag{52}$$

By repeating this calculation method for $(\eta_{mass} - 1)$ number of unit cells, the variation of displacement amplitudes along the barrier is determined. The displacements in the beam to the left and right of the barrier, respectively, are calculated as follows:

$$x < \mathrm{X_L}^-: \qquad W(x) = A_+^L e^{ik_s x} + A_-^L e^{-ik_s x} \tag{53}$$

$$x > \mathrm{X_R}^+: \qquad W(x) = A_+^R e^{ik_s x} \tag{54}$$

## 4. Numerical Results

The behavior of a beam with periodic lumped masses having a unit cell design selected as an example case is discussed in this section. The unit cell consists of two lumped masses and a beam segment, as shown in Figure 1b. With a beam part length of $\ell$ and a shear wave velocity of $\beta$, dimensionless quantities were defined as frequency $\eta = \omega\ell/(2\pi\beta)$, wave number $K_c = k_c\ell$ and foundation parameter $K_f = \bar{k}_f\ell^2$. Furthermore, $m$ was the lumped mass, and $m_{SB} = \rho AL$ was the mass of a pure beam segment, the ratio of the lumped mass to the mass of the beam segment was defined as $\alpha = m/m_{SB}$. If the beam cross-section is considered to be rectangular in the example discussed, the value $\kappa = 5/6 \approx 0.8\dot{3}$ is taken [44].

The results revealing the dispersion properties according to the dimensionless parameters defined for an infinitely long beam resting on an elastic foundation are given for $0 < \eta < 1$ (Figure 7). Figure 7a shows the dimensionless wave number $K_c/\pi$, and Figure 7b,c show the dimensionless phase and group velocities, $C^{ph}/\beta$ and $C^{gr}/\beta$. Dispersion relations of the beam-elastic foundation interaction are given for different $K_f$ values. The foundation stiffness values are taken from the study of Avramidis and Morfidis [45] by referring the "very soft", "medium" and "hard" soil categories. Depending on the $K_f$ value, there is no wave propagation for below the dimensionless critical frequency called the cut-off frequency $\eta_{cr} = \sqrt{K_f}/2\pi$. It is obvious that the cut-off frequency relies on the foundation stiffness and shear wave velocity. This interaction relationship shows that as the foundation stiffness increases, the $\eta_{cr}$ value increases and vice versa.

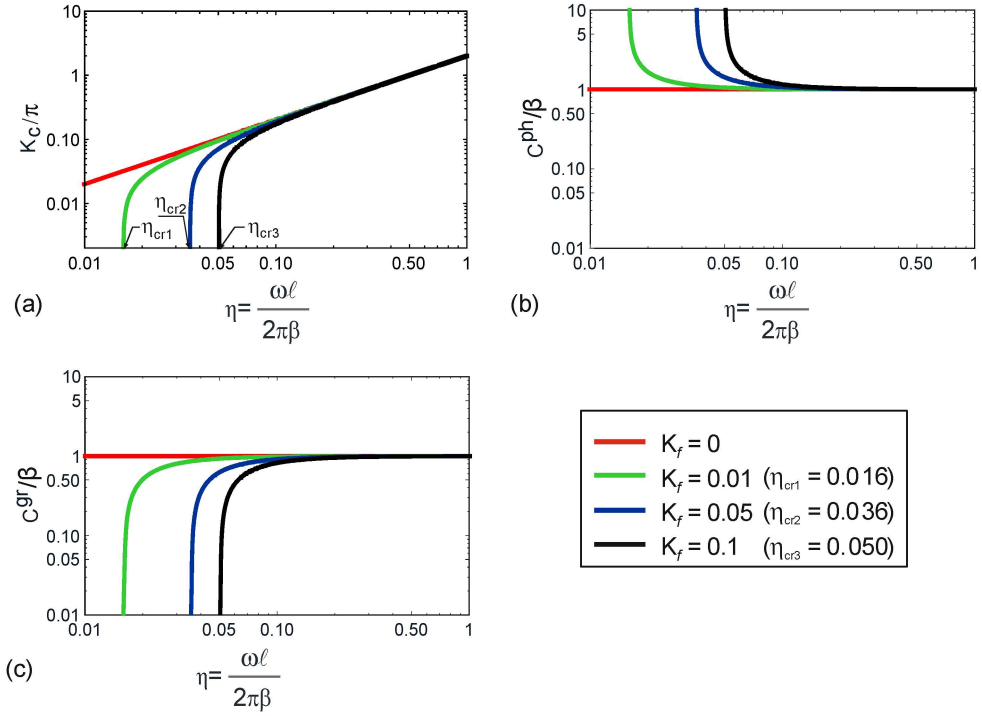


**Figure 7.** Dispersion of infinite beam resting on elastic foundation (no lumped masses); (**a**) the dimensionless wave number; (**b**) the dimensionless phase velocity and (**c**) the dimensionless group velocity.

### *4.1. Frequency Spectrum of the Infinite Periodic Beam*

The frequency spectrum for the shear wave propagating along the infinite periodic beam (Figure 1b) is presented in Figure 8a. Dimensionless frequency $\eta$ and dimensionless wavenumber $K_c$ define the abscissa and the ordinate, respectively. The value $K_c = \pi$ represents the boundary known as the 1st Brillouin zone. Beyond this value, function $K_c = K_c(\eta)$ repeats periodically along the vertical axis. When the frequency spectrum was examined, it was observed that the wave numbers took values for certain frequencies. For example, the second zone contains the $K_c \in (\pi, 2\pi)$ interval. The nonlinearity of the curves indicates that the medium is dispersive. While wave propagation occurs at frequencies corresponding to the real valued wave numbers, this frequency range is called the "pass" band. On the contrary, wave propagation does not occur at frequencies corresponding to complex or pure imaginary wave numbers, and this range is the "stop" band of the dynamic response. The formation of such a banded frequency spectrum arises because of wave interference mechanisms caused by wave scattering and dispersion. If a beam with homogeneous material having the same medium properties is considered and the frequency spectrum is computed to make a comparison with a periodic structure, it is observed that the behavior of the homogeneous beam is not dispersive and thus does not have stop bands. Different $\alpha$ values do not significantly change the pass band initiation except in the 1st Brillouin zone. In the 1st Brillouin zone, on the other hand, the $\eta_{cr}$ value changes depending on the $\alpha$ value, and as the $\alpha$ increases, the $\eta_{cr}$ decreases. In the case of elastic foundation, $\eta_{cr}$ is computed numerically. For the value of $K_f = 0.05$, which $\eta_{cr2}$ values are obtained depending on $\alpha$ are given in Table 1. It is shown that the presence of masses reduces $\eta_{cr}$.

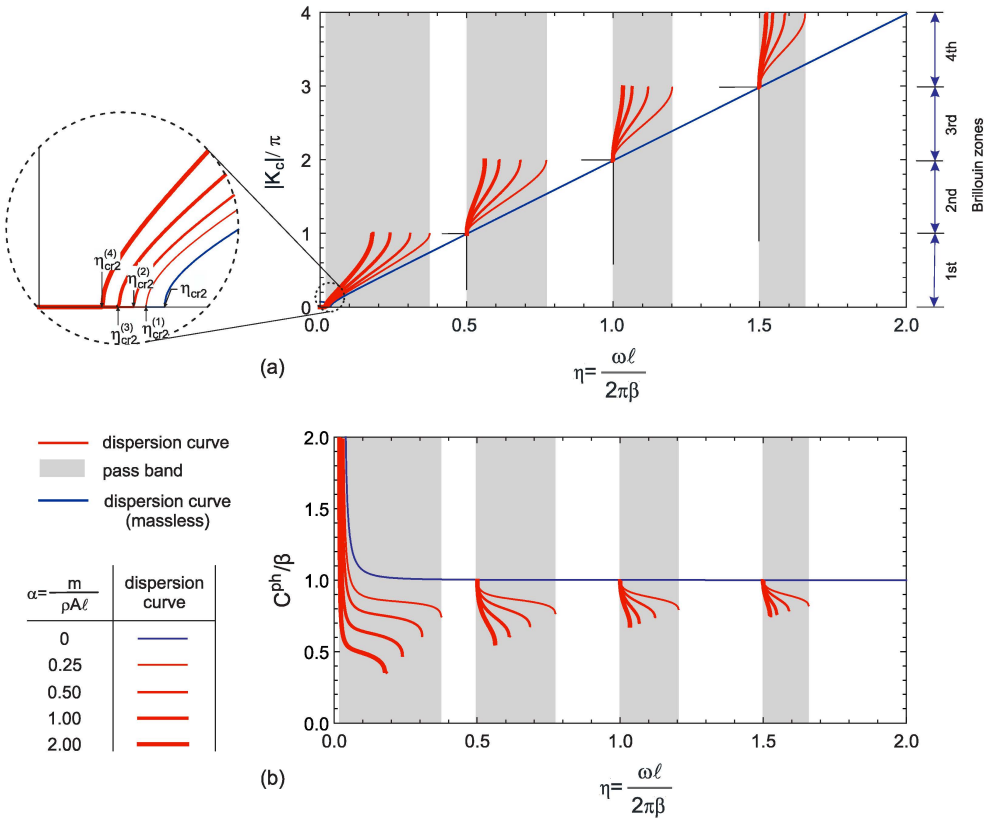


**Figure 8.** Variation of (**a**) dispersion curves, (**b**) phase velocities according to the mass ratio in a one-dimensional periodic structure.

**Table 1.** Variation of cut-off frequency according to the mass ratio in a one-dimensional periodic structure for the value of $K_f = 0.05$.

| $\alpha$ | 0 | 0.25 | 0.5 | 1 | 2 |
|---|---|---|---|---|---|
| $\eta_{cr2}$ | 0.036 | 0.031 | 0.027 | 0.022 | 0.018 |

The variation of the phase velocity in the shear wave along the infinite periodic beam is presented in Figure 8b. These waves propagate only for the frequencies in the pass bands, and the phase velocity changes depending on the frequency and mass ratio. The effect of the lumped masses on the phase velocity in the frequency-dependent pass bands or how they lead to dispersion is observed here. For a nonzero mass ratio ($\alpha > 0$), the waves propagate at velocities slower than that of a shear wave in a homogeneous beam. It is understood that as the mass ratio increases, the pass bands are relatively narrowed, the masses act as a mechanical filter, and the phase velocities also decrease.

The effect of the mass ratio on dispersion, depending on whether there is an elastic foundation or not, is shown in Figure 9. Thus, the effect of the elastic foundation on the periodic beam's behavior has been attempted to be revealed. For this purpose, the situation was examined by taking two different mass ratios, $\alpha = 0.25$ and $\alpha = 2$. The presence of the elastic foundation causes the formation of the low frequency band gap and this band gap also shifts to the left as the magnitude of the masses increases (Figure 9a,b). At high frequencies, the effect of the presence of the elastic foundation on dispersion decreases. This low frequency band gap can be associated with the dynamic properties of elastic metamaterials using elastic resonators, and additionally, these findings are in line with the literature [8,15,20].

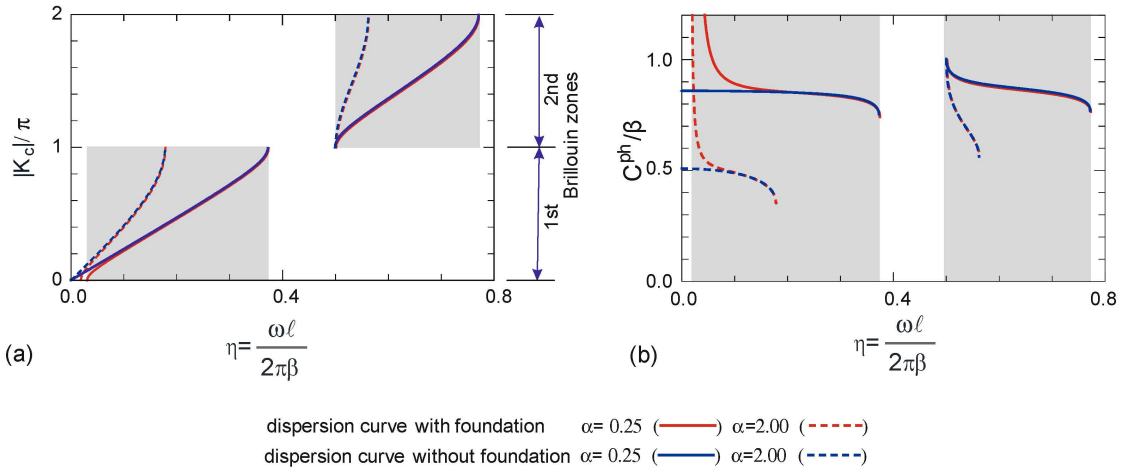


**Figure 9.** Variation of (**a**) dispersion curves, (**b**) phase velocities depending to the mass ratio and elastic foundation parameter for $K_f = 0.05$ and without foundation.

### *4.2. Transmission Response of the Finite Periodic Region in an Infinitely Long Beam*

The effect of periodicity in a finite region in an infinitely long beam will be examined over three different types of barriers, each of which is composed of $N_c$ = 1, 2, 5 cells, respectively, as shown in Figure 10. The transmission function $H_{bar}(\omega)$ given by Equation was evaluated in the same frequency interval as $\eta \in (0, 2)$ provided that the mass ratio $\alpha$ = 0.5 and foundation parameter $K_f$ = 0.05 in the unit cell was taken for each structure discussed in Figure 10, and the results are presented in Figure 11. This equation can be used to compare the frequency band response of an infinite periodic material with the degree of fit of the corresponding transmission response of that material for the periodic structure in a finite region consisting of several cells. Here, it is obviously seen that the frequency response for barriers consisting of 1 or 2 cells does not fit well with the band structure of the infinite periodic unit cell (Figure 11a,b). Nevertheless, the frequency band transmission response of the barrier created with only 5-unit cells are highly compatible with the response corresponding to the infinite medium. While the transmission value is high at pass band frequencies, the transmission values are low at stop band frequencies. These results lead to the conclusion that it is possible to improve or develop the design of structures with finite periodicity using the information obtained from structures with infinite periodicity. Furthermore, it is observed how effective the emerging Bragg scattering mechanism is in the formation of a frequency band structure even at a finite periodicity degree.

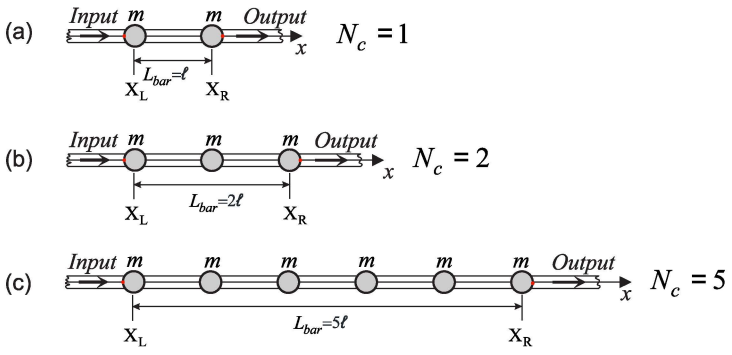


**Figure 10.** Barrier design with (**a**) 1, (**b**) 2, and (**c**) 5 cells in the finite region.

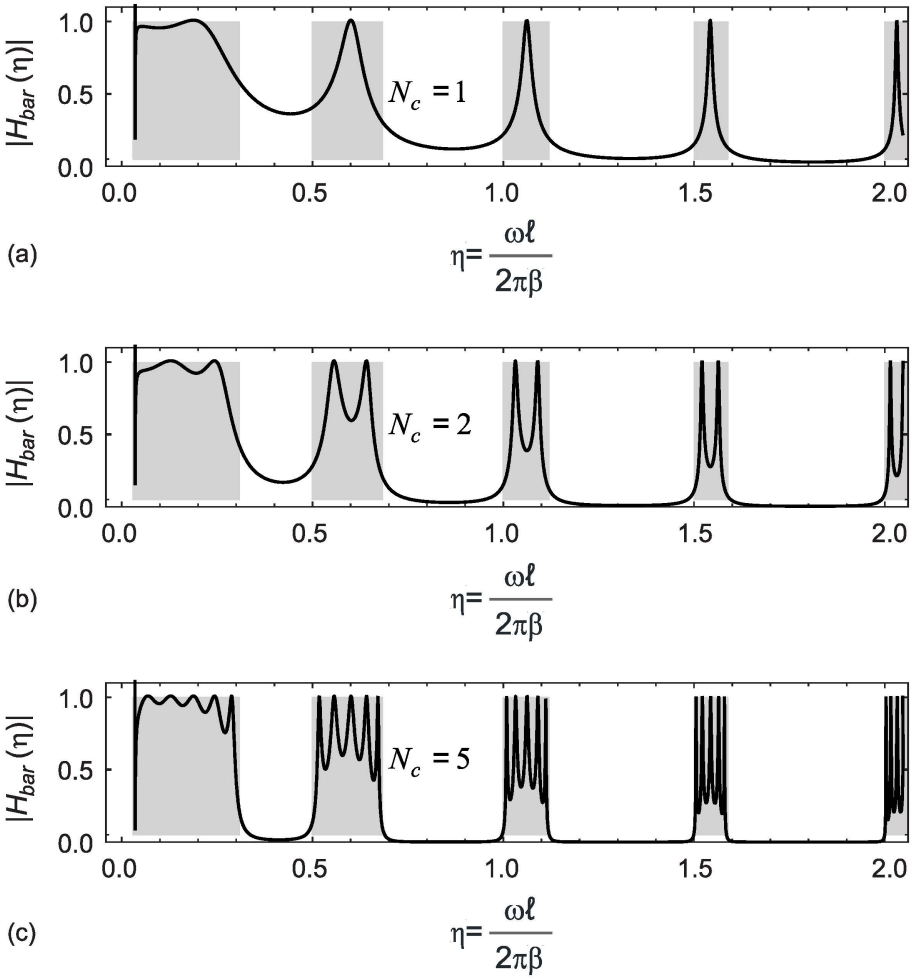


**Figure 11.** Variation of the $H_{bar}(\omega)$ transmission function in the finite region for the mass ratio $\alpha = 1$ and $K_f = 0.05$ according to a (**a**) 1, (**b**) 2, and (**c**) 5-cell barrier.

### *4.3. Displacements in the Finite Periodic Region in an Infinitely Long Beam*

The frequency-dependent variations of the displacement amplitudes associated with wave motion for both the pass band and the stop band of periodic lumped masses in a finite region on a barrier consisting of $N_c = 5$ cells were examined in this section. The fact that the ratio of the lumped mass to the mass of the beam segment was $\alpha = 0.5$ was defined as the "normal state." The variation of the displacements along the $x$-axis for $\alpha = 0.5$ (the normal case), 0.25 (lighter mass than the normal case), 1 (heavy mass), and 2 (even heavier mass) ratios is presented in Figures 12–15. The same foundation parameter is taken for all cases, which is $K_f = 0.05$. The $x$-axis was examined by selecting it to remain within a $2L_{bar} = 10\ell$—long region before the barrier and a $L_{bar} = 5\ell$—long region after the barrier. An incident wave with the $A_+^L = 1$ unit amplitude was taken before the barrier to examine the variation of $W(x)$ along the $x$-axis. Before the barrier, the variation of $W(x)$ shows the interference pattern of the incident and reflected wave. The displacement amplitude was constant since there was a single wave propagating to the right behind the barrier and there was no material damping.

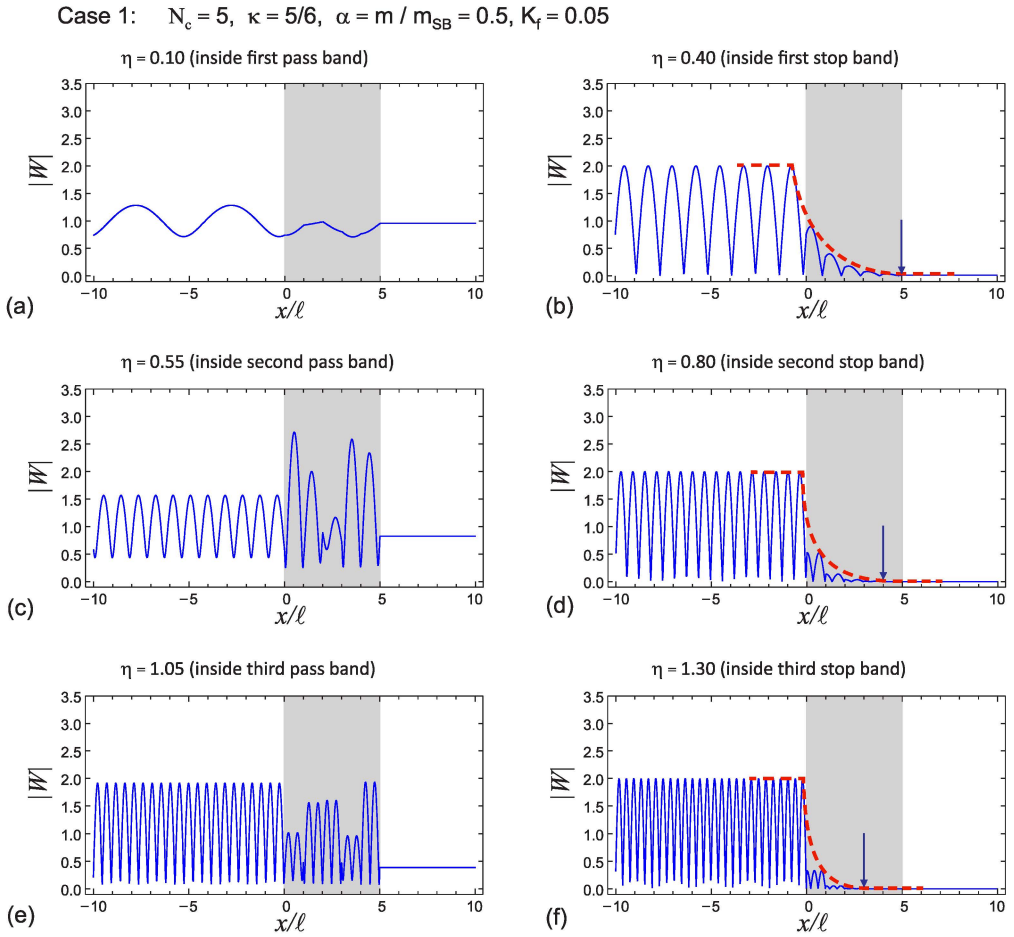


**Figure 12.** Variation of displacement amplitudes under the barrier effect in the finite region for Case 1.

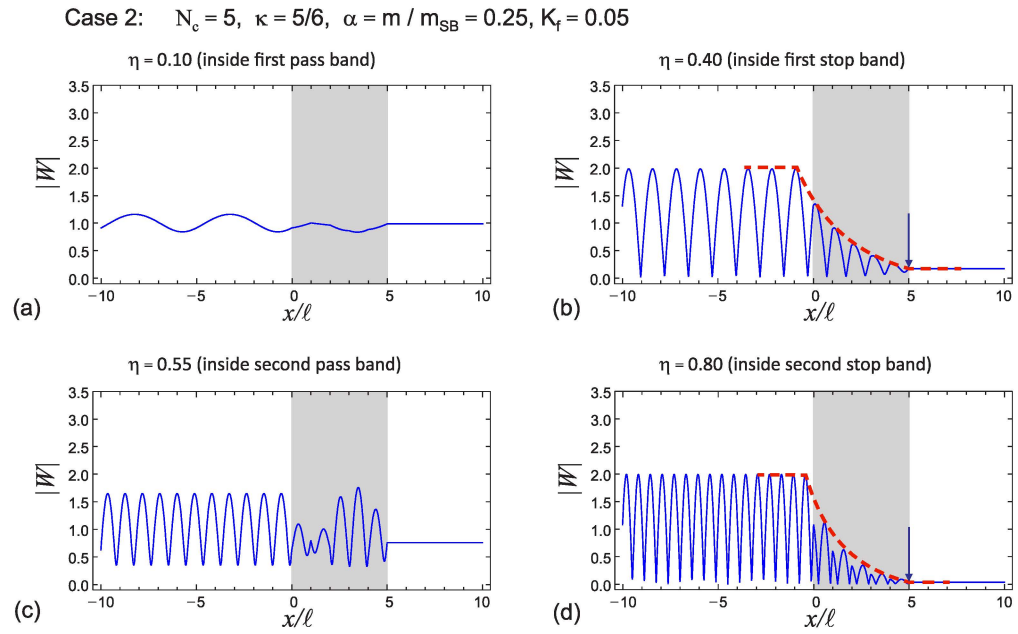


**Figure 13.** Variation of displacement amplitudes under the barrier effect in the finite region for Case 2.

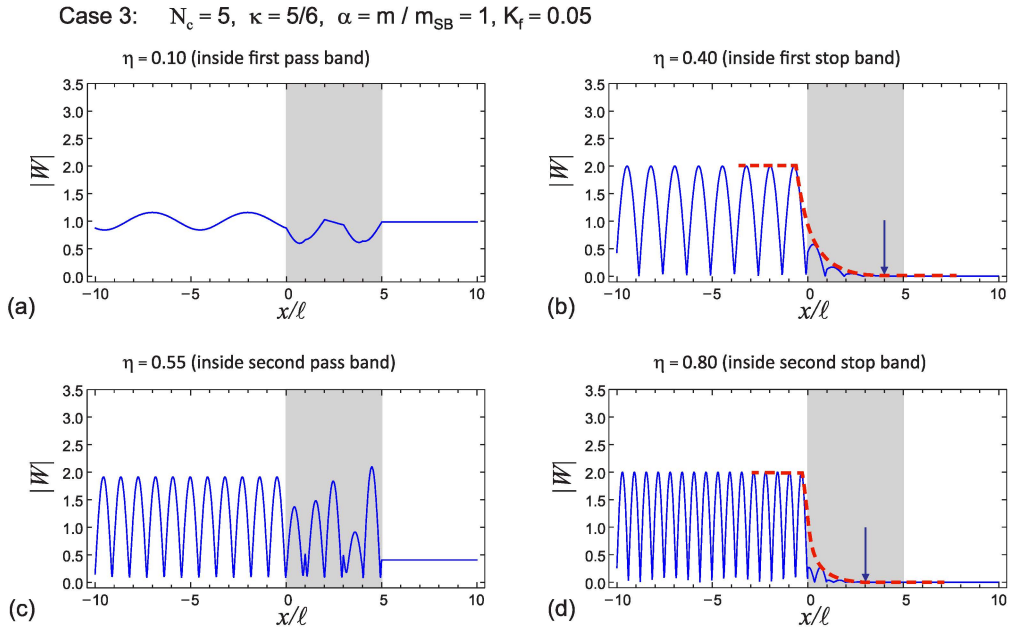


**Figure 14.** Variation of displacement amplitudes under the barrier effect in the finite region for Case 3.

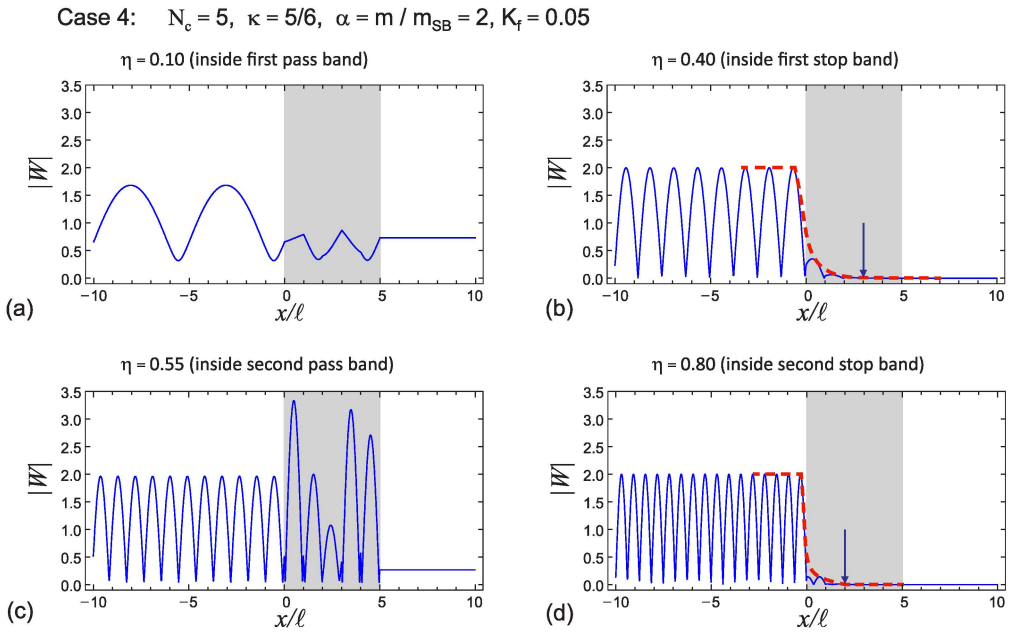


**Figure 15.** Variation of displacement amplitudes under the barrier effect in the finite region for Case 4.

When Case 1 was examined, it was observed that the amplitude was close to 1 for the frequency $\eta \in (0, 0.7)$ in the first two pass bands and close to 0.5 in the third pass band (Figure 12a,c,e). While the low-frequency incident wave was transmitted almost as it was, although amplitudes increased inside the barrier at high frequencies, the displacements had much less amplitude than 1 when they passed the barrier. For the frequency values selected in the first three stop bands, the amplitudes quickly went to zero when they passed the barrier (Figure 12b,d,f). While the displacement amplitude in the first stop band approached zero at the end of the barrier, it became zero at the $\frac{3}{5}L_{bar}$ of barrier length in the second stop band and zero at the $\frac{3}{5}L_{bar}$ of barrier length in the third stop band.

When Case 2 was examined, the amplitude was close to 1 for the frequency $\eta \in (0, 0.77)$ in the first two pass bands (Figure 13a,c). For low frequency values in the pass band, the

incident wave was transmitted as it was, and the barrier had almost no effect. For the selected frequency values in the stop band, the amplitudes quickly went to zero when they passed the barrier (Figure 13b,d). For the "lighter mass" case, the displacement amplitude in the first two stop bands approached or became zero, respectively, at the end of the barrier. It was observed that the effect of the masses was relatively less compared to the "normal state".

When the "heavy mass" case was examined, the amplitude was very close to 1 for the frequency selected in the first pass band, and the incident wave was transmitted as it was. However, in the second pass band, the post-barrier amplitude decreased below 0.5 with the effect of the masses (Figure 14a,c). Although the amplitudes increased inside the barrier at high frequencies in the pass band, it was observed that the displacements had an amplitude much less than 0.5 when they passed the barrier. For the frequency values selected in the first two stop bands, it was found that the amplitudes quickly went to zero inside the barrier (Figure 14b,d). The displacement amplitude became zero at the $\frac{4}{5}L_{bar}$ parts of the barrier in the first stop band and at the $\frac{3}{5}L_{bar}$ parts of the barrier in the second stop band.

When the "very heavy mass" case was examined, it was observed that the amplitude was close to 1 for the frequency selected in the first pass band and that the post-barrier amplitude decreased below 0.5 with the effect of the masses for the frequency selected in the second pass band (Figure 15a,c). It was revealed that although the amplitudes increased inside the barrier for high frequencies in the pass band, the displacements decreased when they passed the barrier. It was observed that the displacement amplitude decreased rapidly until it reached the $\frac{3}{5}L_{bar}$ part of the barrier in the first stop band and the $\frac{2}{5}L_{bar}$ part of the barrier in the second stop band, and it went to zero (Figure 15b,d).

## 5. Discussion and Conclusions

In this study, the dispersion phenomenon occurring in an infinitely long shear beam with a periodic lumped mass and resting on an elastic foundation is investigated. The influence of the periodically located lumped masses (in a finite region) on the wave attenuation is examined through the displacement response of the beam. The combination of perfectly bonded lumped mass and a beam segment is used as a unit cell for the dispersion analysis. The analytical solution is achieved by using the Floquet Theory and adopting the Transfer Matrix method. A wave-based approach is implemented to obtain the reflection and transmission of waves at the boundaries of the unit cell, thus, the effect of periodicity in the finite region on wave transmission is examined.

The main results obtained can be listed as follows. The periodically placed lumped masses revealed a banded structure in the frequency spectrum of the infinite beam. In case of a homogeneous beam resting on an elastic foundation, the cut-off frequency is a constant depending on the stiffness of the foundation. On the other hand, the cut-off frequency decreases monotonically when the magnitude of the masses increases. It is shown that the wave propagation occurs only in the pass bands, and the phase velocities decreases with increasing magnitude of the masses. Furthermore, stop bands blocks wave energy transmission, and periodic masses acts as a mechanical filter. The relative increase in the magnitude of lumped mass leads to narrowing of the pass bands and a decrease in phase velocities.

In the case of a periodic lumped mass in the finite region, the dynamic transmission response is obtained through the ratio of the amplitude of the incident wave in front of the barrier and the amplitude of the wave passing behind the barrier. Even if a region of a limited number of unit cells are selected, i.e., 5-unit cells, it acts as a barrier, namely, the transmission values decrease at stop band frequencies. Depending on the mass ratio, the displacement amplitude behind the barrier is close to 1 at low frequency values in the pass bands and well below 1 at high frequencies. For stop bands, the displacement amplitude inside the barrier quickly approaches to zero.

The results given in terms of the present model include a limited frequency range and cell number and are valid under some assumptions. In this sense, this approach may

present an engineering sense for practical calculations, as it reveals important information on the influence of the infinite and finite periodicity. The responses that are close to the responses of infinite periodicity were achieved by a finite periodic design. As a result, it can be concluded that vibration reduction can be acquired by including a periodicity in the design despite the absence of dampers.

**Funding:** This research received no external funding.

**Institutional Review Board Statement:** Not applicable.

**Informed Consent Statement:** Not applicable.

**Data Availability Statement:** Not applicable.

**Acknowledgments:** The author would like to thank Hasan Engin for critical reading and for sharing his valuable views and comments during the preparation of the manuscript. The author is also grateful to the anonymous reviewers for their insightful comments.

**Conflicts of Interest:** The author declare no conflict of interest.

## References

1. Hussein, M.I.; Leamy, M.J.; Ruzzene, M. Dynamics of phononic materials and structures: Historical origins, recent progress, and future outlook. *Appl. Mech. Rev.* **2014**, *66*, 040802. [CrossRef]
2. Hussein, M.I.; Hulbert, G.M.; Scott, R.A. Dispersive elastodynamics of 1D banded materials and structures: Analysis. *J. Sound Vib.* **2006**, *289*, 779–806. [CrossRef]
3. Brillouin, L. *Wave Propagation in Periodic Structures: Electric Filters and Crystal Lattices*, 2nd ed.; Dover: New York, NY, USA, 1953.
4. Yong, Y.; Lin, Y.K. Propagation of decaying waves in periodic and piecewise periodic structures of finite length. *J. Sound Vib.* **1989**, *129*, 99–118. [CrossRef]
5. Mead, D.M. Wave propagation in continuous periodic structures: Research contributions from Southampton, 1964–1995. *J. Sound Vib.* **1996**, *190*, 495–524. [CrossRef]
6. Liu, L.; Hussein, M.I. Wave motion in periodic flexural beams and characterization of the transition between Bragg scattering and local resonance. *J. Appl. Mech.* **2012**, *79*, 011003. [CrossRef]
7. Sigalas, M.M.; Economou, E.N. Elastic and acoustic wave band structure. *J. Sound Vib.* **1992**, *158*, 377–382. [CrossRef]
8. Zhao, P.; Zhang, K.; Deng, Z. Size effects on the band gap of flexural wave propagation in one-dimensional periodic micro-beams. *Compos. Struct.* **2021**, *271*, 114162. [CrossRef]
9. Baz, A. Active Control of periodic structures. *J. Vib. Acoust* **2001**, *123*, 472–479. [CrossRef]
10. Jensen, J.S. Phononic band gaps and vibrations in one- and two-dimensional mass–spring structures. *J. Sound Vib.* **2003**, *266*, 1053–1078. [CrossRef]
11. Goto, A.M.; Nóbrega, E.D.; Pereira, F.N.; Dos Santos, J.M.C. Numerical and experimental investigation of phononic crystals via wave-based higher-order rod models. *Int. J. Mech. Sci.* **2020**, *181*, 105776. [CrossRef]
12. Santos, R.B.; Carneiro Junior, J.P.; Gonsalez-Bueno, C.G.; de Lucca, B.S.; Bueno, D.D. On the number of cells for flexural vibration suppression in periodic beams. *Meccanica* **2021**, *56*, 2813–2823. [CrossRef]
13. Lamprea-Pineda, A.C.; Connolly, D.P.; Hussein, M.F. Beams on elastic foundations—A review of railway applications and solutions. *Transp. Geotech.* **2022**, *33*, 100696. [CrossRef]
14. Tassilly, E. Propagation of bending waves in a periodic beam. *Int. J. Eng. Sci.* **1987**, *25*, 85–94. [CrossRef]
15. Yu, D.; Wen, J.; Shen, H.; Xiao, Y.; Wen, X. Propagation of flexural wave in periodic beam on elastic foundations. *Phys. Lett. A* **2012**, *376*, 626–630. [CrossRef]
16. Han, L.; Zhang, Y.; Li, X.; Jiang, L.; Chen, D. Flexural vibration reduction of hinged periodic beam–foundation systems. *Soil Dyn. Earthq. Eng.* **2015**, *79*, 1–4. [CrossRef]
17. Xiang, H.-J.; Shi, Z.-F. Vibration attenuation in periodic composite Timoshenko beams on Pasternak foundation. *Struct. Eng. Mech.* **2011**, *40*, 373–392. [CrossRef]
18. Liu, X.; Shi, Z. WFQEM-based perturbation approach and its applications in analyzing nonlinear periodic structures. *Math. Meth. Appl. Sci.* **2017**, *40*, 3079–3091. [CrossRef]
19. Liu, X.; Shi, Z.; Mo, Y.L. Effect of initial stress on periodic Timoshenko beams resting on an elastic foundation. *J. Vib. Control* **2017**, *23*, 3041–3054. [CrossRef]
20. Ding, W.; Hollkamp, J.P.; Patnaik, S.; Semperlotti, F. On the fractional homogenization of one-dimensional elastic metamaterials with viscoelastic foundation. *Arch. Appl. Mech.* **2022**. [CrossRef]
21. Leckie, F.; Pestel, E. Transfer-matrix fundamentals. *Int. J. Mech. Sci.* **1960**, *2*, 137–167. [CrossRef]
22. Uhrig, R. The transfer matrix method seen as one method of structural analysis among others. *J. Sound Vib.* **1966**, *4*, 136–148. [CrossRef]

23. Lin, Y.K.; Donaldson, B.K. A brief survey of transfer matrix techniques with special reference to the analysis of aircraft panels. *J. Sound Vib.* **1969**, *10*, 103–143. [CrossRef]
24. Yu, D.; Liu, Y.; Wang, G.; Zhao, H.; Qiu, J. Flexural vibration band gaps in Timoshenko beams with locally resonant structures. *J. Appl. Phys.* **2006**, *100*, 124901. [CrossRef]
25. Chen, T. Investigations on flexural wave propagation of a periodic beam using multi-reflection method. *Arch. Appl. Mech.* **2013**, *83*, 315–329. [CrossRef]
26. Gu, J.; Rui, X.; Chen, G.; Zhou, Q.; Yang, H. Distributed parallel computing of the recursive eigenvalue search in the context of transfer matrix method for multibody systems. *Adv. Mech. Eng.* **2016**, *8*, 168781401668073. [CrossRef]
27. Banerjee, A. Non-dimensional analysis of the elastic beam having periodic linear spring mass resonators. *Meccanica* **2020**, *55*, 1181–1191. [CrossRef]
28. Mace, B.R. Wave reflection and transmission in beams. *J. Sound Vib.* **1984**, *97*, 237–246. [CrossRef]
29. Mei, C.; Mace, B.R. Wave reflection and transmission in Timoshenko beams and wave analysis of Timoshenko beam structures. *J. Vib. Acoust.* **2005**, *127*, 382–394. [CrossRef]
30. Ekhteraei Toussi, H.; Sadeghian, M. Frequency analysis for a Timoshenko beam located on an elastic foundation. *Int. J. Eng.* **2011**, *24*, 87–105.
31. Miller, D.W.; Flotow, A. von. A travelling wave approach to power flow in structural networks. *J. Sound Vib.* **1989**, *128*, 145–162. [CrossRef]
32. Saeed, H.M.; Vestroni, F. Simulation of combined systems by periodic structures: The wave transfer matrix approach. *J. Sound Vib.* **1998**, *213*, 55–74. [CrossRef]
33. Leamy, M.J. Exact wave-based Bloch analysis procedure for investigating wave propagation in two-dimensional periodic lattices. *J. Sound Vib.* **2012**, *331*, 1580–1596. [CrossRef]
34. Xu, X.; Zuo, S.; Zhang, K.; Hu, G. Wave-based transfer matrix method for dynamic response of large net structures. *J. Sound Vib.* **2018**, *433*, 265–286. [CrossRef]
35. Balaji, N.N.; Brake, M.R.W.; Leamy, M.J. Wave-based analysis of jointed elastic bars: Nonlinear periodic response. *Nonlinear Dyn.* **2022**, *110*, 2005–2031. [CrossRef]
36. Lv, H.; Zhang, Y. A wave-based vibration analysis of a finite Timoshenko locally resonant beam suspended with periodic uncoupled force-moment type resonators. *Crystals* **2020**, *10*, 1132. [CrossRef]
37. Lv, H.; Zhang, Y. Wide band-gaps in finite Timoshenko locally resonant beams carrying periodic separated force and moment resonators: Forced vibration analysis based on an exact wave-based approach. *J. Vib. Eng. Technol.* **2021**, *9*, 1109–1121. [CrossRef]
38. Lv, H.; Li, S.; Huang, X.; Yu, Z. Vibration analysis of a finite lightweight locally resonant beam suspended with periodic force-moment-type resonators inside using an exact wave-based approach. *Symmetry* **2022**, *14*, 1542. [CrossRef]
39. Doyle, J.F. *Wave Propagation in Structures: An FFT-Based Spectral Analysis Methodology*; Springer: New York, NY, USA, 1989. ISBN 9781468403442.
40. Wolf, J.P. *Dynamic Soil-Structure Interaction*; Prentice-Hall: Englewood Cliffs, NJ, USA; London, UK, 1985. ISBN 0132215659.
41. Yu, C.-P.; Roesset, J.M. Dynamic stiffness matrices for linear members with distributed mass. *J. Appl. Sci. Eng.* **2001**, *4*, 253–264. [CrossRef]
42. Dai, W.; Yu, C.P.; Roesset, J.M. Dynamic stiffness matrices for analyses in the frequency domain. *Comput.-Aided Civ. Eng.* **2007**, *22*, 265–281. [CrossRef]
43. Fukuwa, N.; Matsushima, S. Wave dispersion and optimal mass modelling for one-dimensional periodic structures. *Earthq. Engng. Struct. Dyn.* **1994**, *23*, 1165–1180. [CrossRef]
44. Kaneko, T. On Timoshenko's correction for shear in vibrating beams. *J. Phys. D Appl. Phys.* **1975**, *8*, 1927–1936. [CrossRef]
45. Avramidis, I.E.; Morfidis, K. Bending of beams on three-parameter elastic foundation. *Int. J. Solids Struct.* **2006**, *43*, 357–375. [CrossRef]